Archives of Waste Management and Environmental Protection

Archiwum Gospodarki Odpadami i Ochrony Środowiska

ISSN 1733-4381, vol. 14, issue 2 (2012), p.51-62

http://awmep.org

Influences of process parameters on optimal working conditions for catalyst carriers in the selective oxidation or incineration of hydrocarbons

Waldemar KRAJEWSKI [1,3], Krystian KALINOWSKI [2], Zbigniew NAJZAREK [3]

[1] *Institute of Chemical Engineering PAS, 5 Baltycka St., 44-100 Gliwice, tel. :32-23-10-811, e-mail: wkrajew@iich.gliwice.pl*

[2] *Silesian University of Technology, Department of Electrical Engineering and Control in Mining, 2 Akademicka St., 44-100 Gliwice, tel.: 32-23-71-250, e-mail: krystian.kalinowski@ polsl.pl*

[3] *Opole University of Technology, Department of Applications of Chemistry and Mechanics, 5 Mikolajczyka St., 45-271 Opole, tel.:77-45-38-447, e-mail: z.najzarek@po.opole.pl*

Abstract

Heat-flow characteristics for the eleven catalyst carriers are presented. Within these carriers, optimal values of Bejan number were determined for which the maximal ratio of Nusselt number to the dimensionless entropy generation rate attained its maximum. These number values were determined under sequential changing of the bed length, the bed outlet pressure, the air temperature at the bed inlet, and the wall temperature. Correlations are given for the optimal Bejan number, depending on these process parameters. Such correlations are also presented for the optimal Reynolds number, as well as for the maximal ratio of Nusselt number to the dimensionless entropy generation rate.

Keywords: heat transfer, Bejan number, entropy generation

Streszczenie

Wpływ parametrów procesu na optymalne warunki pracy nośników katalizatorów stosowanych w procesach selektywnego utleniania i dopalania węglowodorów

Podano charakterystyki cieplno–przepływowe dla 11 nośników katalizatora. Dla tych nośników wyznaczono optymalne wartości liczb Bejana przy których stosunek liczb Nusselta do bezwymiarowej szybkości generacji entropii osiąga wartość maksymalną. Te liczby wyznaczono zmieniając kolejno długość złoża, ciśnienie na wylocie ze złoża, temperaturę wlotową powietrza na złoże i temperaturę ścianki. Podano korelacje na optymalne liczby Bejana w zależności od parametrów procesu. Przedstawiono również takie korelacje na optymalne liczby Reynoldsa oraz wartości maksymalne stosunku liczb Nusselta do bezwymiarowej szybkości generacji entropii.

Słowa kluczowe: przepływ ciepła, liczba Bejana, generacja entropii.

1. Introduction

Increasing air pollution remains still unsolved problem. Catalytic afterburning is mostly used to try to neutralize harmful waste gases of chemical and power industries, as well as in transport. Significant progress in catalyst development allows to reduce the afterburning temperature and to cut down the contact time at a catalyst. Catalysts are mostly settled on ceramic beds or on the surface of monoliths [1]. Unfortunately ceramic beds have great mass, and using of very small bed channels causes excessive increase in flow resistance. On the other hand, in the monoliths a laminar flow arises, what significantly reduces the diffusion rate of reactants into catalyst surface, and hence the afterburning efficiency falls. Developing of new types of chromium-nickel steel 00H20J5 gives abilities to construct new structural catalyst carriers, in which significant ceramic bed and monolith defects have been removed.

In research described in study [2] several carriers are presented, for which heat exchange and flow resistance measurements were carried out. Heat and flow characteristics for these carriers are presented in the table 1.1. In

the column 1 carrier number is quoted, in the second its construction is described, in the third – its unitary surface is presented, and in the fourth – bed porosity. In the fifth column correlation for Nusselt number, and in the sixth - Fanning friction factor is quoted. Measurements were carried out in a tube of D= 25.4 mm diameter and 0.6 m height. The measurement way is in details described in the study [2]. Air was being pumped through the tube. Analytical diameter of D= 25.4 mm was assumed and Reynolds number was defined by the formula: Re = GD/ η. Reynolds numbers were being changed in the range of 1000-10000. During these measurements the inlet air temperature was $T_{in,o}$ =315K, tube wall temperature was $T_{w,o}$ =395K and the outlet pressure was p_o=101.325kPa. A vanadium phosphorus oxide catalyst was placed on one of the selected carriers (carrier no. 7) made of chromium-nickel steel 00H20J5 and a process of selective n-butane oxidation into maleic anhydride was carried out on it. This process is in detail described in the study [3]. This confirms the ability of applying presented metal carriers in chemical compounds oxidation and afterburning processes.

In the next study [4] organic compounds afterburning on a monolith, made of 00H20J5 steel foil, and covered with platinic or palladic catalyst is described. This confirms the ability of applying this steel as a catalyst carrier and makes afterburning on them such compounds as benzene, toluene, n-heptane, etc possible.

By great quantity of various catalyst carriers arises a problem, how to select the best type by given process conditions. Furthermore, the best solution should be substantiated. Such abilities gives selection of carriers, those have the highest heat exchange intensity and simultaneously minimal entropy generation rate. Carriers with maximal ratio of Nusselt numbers to the dimensionless entropy generation rate have been searching. By this criterion, obtained calculation results can be easily recalculated for other cases, e.g. considering exergies or minimum economic costs [5].

Table 1.1. The heat-flow characteristic of the carriers

No	Carrier	a m^2/m^3	ε m^3/m^3	Fanning friction factor	Nusselt number
1	Spiral fin ϕ=24.3 round the pipe ϕ =10. Fin screw unit h=7.5mm, thickness 0.5mm.	258	0.803	$f=1116.9\ Re^{-0.46}$	$Nu=0.0538\ Re^{0.930}$
2	Metal Raschig rings ϕ 5.1x5x0.25mm, randomly packed	905	0.892	$f=190.4\ Re^{-0.285}$	$Nu=0.0604\ Re^{0.927}$
3	Single helical surface made of wire with axial insert of metal foil half-rings ϕ_i/ϕ_e =7.8/24.4, t=0.05.	408	0.946	$f=87.53\ Re^{-0.184}$	$Nu=0.0252\ Re^{1.017}$
4	Metal rosettes (20 leafs ϕ= 26, h= 22, t= 0,05) with a drop-like core (ϕ=11.8, h=19.1) alternately packed with rings (ϕ_i/ϕ_e =16/25.3, t= 0.05) .	857	0.858	$f=80.09\ Re^{-0.279}$	$Nu=0.0442\ Re^{0.94}$
5	Two metal rosettes (20 leafs ϕ= 26, h=10, t= 0.05) alternately packed with rings (ϕ_i/ϕ_e =16/25.3, t= 0.05) .	963	0.976	$f=44.13\ Re^{-0.171}$	$Nu=0.0295\ Re^{1.004}$
6	Two metal rosettes (20 leafs ϕ= 26, h=10, t= 0.05) alternately packed with U-shaped rings type A (ϕ_i/ϕ_e=14.1/24.3, h=2.0, t= 0.3)	896	0.974	$f=14.45Re^{-0.118}$	$Nu=0.0755\ Re^{0.873}$
7	Metal rosettes (20 leafs ϕ=26, h=10, t= 0.05) alternately packed with U-shaped rings type B (ϕ_i/ϕ_e=11.8/22.4, h=2.2, t=0.3)	918	0.956	$f=62.34\ Re^{-0.216}$	$Nu=0.156\ Re^{0.820}$

No	Carrier	a m^2/m^3	ε m^3/m^3	Fanning friction factor	Nusselt number
9	Metal rings with internal leaf ϕ4.5x5x0.05mm, randomly packed	1504	0.925	$f=209.5\ Re^{-0.298}$	$Nu=0.018\ Re^{1.058}$
10	Ceramic Rashig rings with rounded edges ϕ7x7x1.5 mm, randomly packed	750	0.537	$f=116.67Re^{-0.272}$	$Nu=0.0933\ Re^{0.864}$
11	Ceramic half-rings ϕ10x6x2mm, randomly packed	690	0.546	$f=155.47Re^{-0,262}$	$Nu=0.0217\ Re^{1.048}$

Descriptions: a - carrier specific surface; ε - porsity; ϕ - dimension, mm; ϕ_i , ϕ_e – internal, external dimension, mm; t – thickness of the carrier metal foil, mm; h – height or helical screw unit, mm.

2. Determining of maximal ratio of Nusselt number values to the dimensionless entropy generation rate

According to the study [6], the entropy generation rate is expressed by following equation:

$$\dot{S} = \dot{S}' + \dot{S}'' = \frac{32\dot{m}^3 fL}{\rho^2\pi^2 D^5 T_m} + \frac{(q^2/L)D}{4T_m{}^2 \dot{m} c_p St} \tag{2.1}$$

In this equation, the first and second terms denote the entropy generation rate with the flow resistance and with the heat exchange, respectively.

Bejan number (2.2) and the dimensionless ratio of entropy generation rate (2.3) have been introduced:

$$Be = \dot{S}''/(\dot{S}' + \dot{S}'') \tag{2.2}$$

$$\dot{S}''' = \dot{S}/\dot{m}c_p \tag{2.3}$$

Ratio values of Nusselt number Nu to the dimensionless entropy generation rate Nu/ $\dot{S}'''$ have been set out based on the correlations for Nusselt number and the flow resistance coefficient quoted in table 1.1. These calculations were carried out under the inlet air

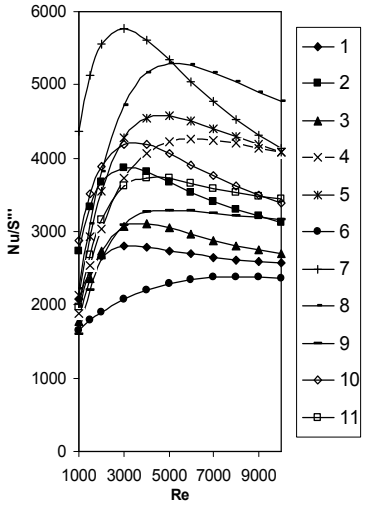

Fig. 2.1. Dependence of the dimensionless term Nu/S''' on Reynolds number for the eleven carriers. The inlet air temperature 315 K. The outlet air pressure 101.325 kPa. The tube wall temperature 398 K. The tube length 0.6m. The tube diameter 25.4 mm. The carriers are described in table 1.1

temperature $T_{in,o}$ =315 K, the tube wall temperature $T_{w,o}$=395 K and the pressure at the bed outlet p_o=101.325 kPa.

Dependences of the ratio Nu/ $\dot{S}^{'''}$ on Reynolds number for the 11 carriers have been obtained, and are presented on fig. 2.1a. Succeeding carriers from table 1.1 are expressed by symbols shown on that figure. For every carrier exist maximal ratio Nu/$S^{'''}$ and it is marked by sign Nu/S'''_{max} . The optimum Reynolds number value Re_{opt} corresponds to this maximum ratio value. This ratio is maximal for carrier no. 7 consisting of rosettes and U-shaped rings type B, than carrier no. 8 followed by carriers nos. 6, 5, 4, 10, 2, 11, 9, 3, and 1. Thus, the sequence of the best carriers were established. Related graphs in the vicinity of maximal points reveal small curvature. For all the carriers, an average reduction of Nu/$S^{'''}$ value from the maximum for 5% corresponds an alternation of the optimum Reynolds number value in the range from -37% to +63%. Hence, in the vicinity of Re_{opt} the carriers work almost optimally. So, it is appropriate to show Nu/S'''_{max} values for all the carriers.

Fig. 2.2.b presents the relation between Bejan number and Reynolds number for the eleven carriers. These carriers are characterized in fig. 2.1 and in table 1.1.

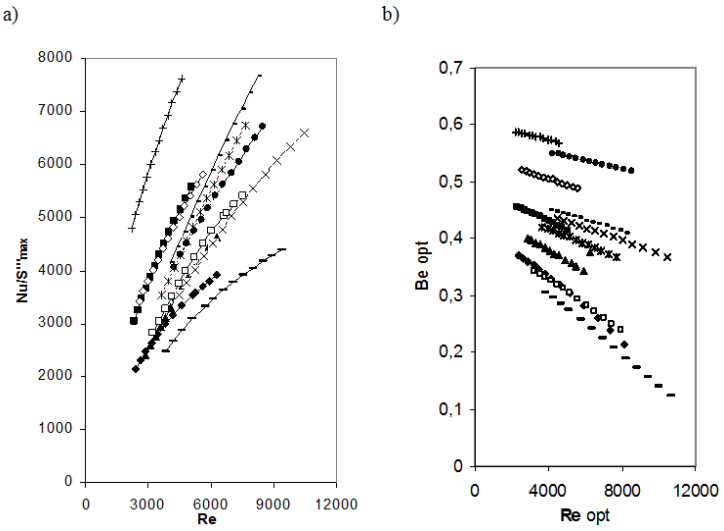

Fig. 2.2. Dependence of maximal value of the dimensionless term Nu/S'''_{max} or optimal Bejan number Be_{opt} on optimal Reynolds number, respectively, for the eleven carriers under variation of the outlet air pressure. The

inlet air temperature 315K. The tube wall temperature 398 K. The tube length 0.6 m. The tube diameter 25.4 mm. The carriers are described in table 1.1 and fig. 2.1. Increasing values of the optimal Reynolds number Re_{opt} were obtained changing successively the dimensionless outlet air pressure (P) for: 0.80, 0.85, 0.90, 0.95, 1.00, 1.05, 1.10, 1.15, 1.20, 1.25, 1.30, 1.35 and 1.40. a) Relationship between the dimensionless term Nu/S'''_{max} and optimal Reynolds number. b) Relationship between the optimal Bejan number Be_{opt} and the optimal Reynolds number Re_{opt} .

3. Dependence of optimal Bejan number values Be_{opt} on the process parameters

Also the process parameters such as the pressure at bed outlet, the bed length, the inlet air temperature and the wall temperature have influenced the maximal values of Nu/S'''_{max}. A dimensionless pressure was introduced: $P=p/p_o$, where p_o =101.325 kPa. The values of Nu/S'''_{max} were calculated one by one under the dimensionless pressures P=0.8, 0.85, 0.9, 0.95, 1.00, 1.05, 1.10, 1.15,1.20, 1.25, 1.30, 1.35, and 1.40 for the eleven carriers. These

Table 3.1. The process parameters derived from Be_{opt} and Re_{opt} values that are presented in figs. 2.1b -3.2. The following values of the dimensionless outlet air pressure P were introduced: 0.80, 0.85, 0.90, 0.95, 1.00, 1.05, 1.10, 1.15, 1.20, 1.25, 1.30, 1.35, and 1.40.

No	No. fig.	T_{in}	T_w	L
		K	K	m
1	2.2b	315	398	0.6
2	3.1a-d	315	398	0.8, 1.0, 1.2, 1.4
3	3.2a,b	335, 355	398	0.6
4	3.2b,c	315	378, 358	0.6

Table 3.2. The remaining process parameters for which were determined optimal values of Reynolds and Bejan numbers, Re_{opt} and Be_{opt} , as well as optimal values of dimensionless term Nu/S'''_{max}.

No	T_{in}	T_w	L
	K	K	m
1	315	398	0.7, 0.9
2	335, 355	398	0.7, 0.8, 0.9, 1.0, 1.2
3	315	378, 358	0.7, 0.8, 0.9, 1.0, 1.2
4	355	438	0.6, 0.7, 0.8, 0.9, 1.0, 1.2
5	395	478	0.6
6	435	518	0.6
7	475	558	0.6
8	515	598	0.6
9	555	638	0.6

calculation results are shown in fig.3.1. The individual carriers are marked there by symbols given in fig. 2.1a.

Curves were drawn across points thus calculated, and diminished slopes were obtained. The left extreme points on these curves were set out by P= 0.8, and the right extreme ones by P=1,4. When the dimensionless pressure rises, the optimal Be_{opt} values diminishes,

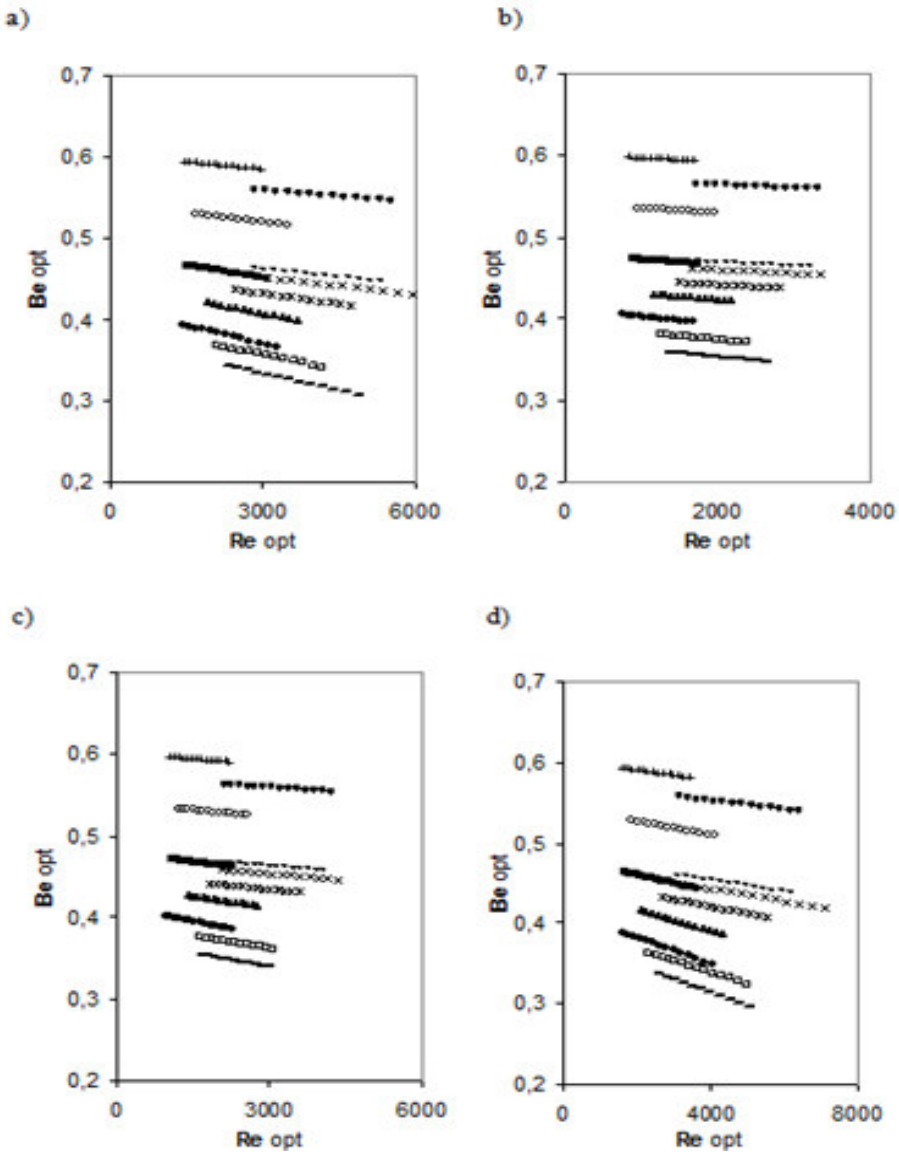

Fig. 3.1. Dependence of optimal Bejan number (Be_{opt}) on Reynolds number through the eleven carriers under conditions of variable pressure at the outlet air. The carrier description are presented in table 1.1 and in fig. 2.1. The process parameters are given by legend of fig. 2.1., however bed length was changed successively for: a)0.8m, b)1.0m, c)1.2m, d)1.4m.

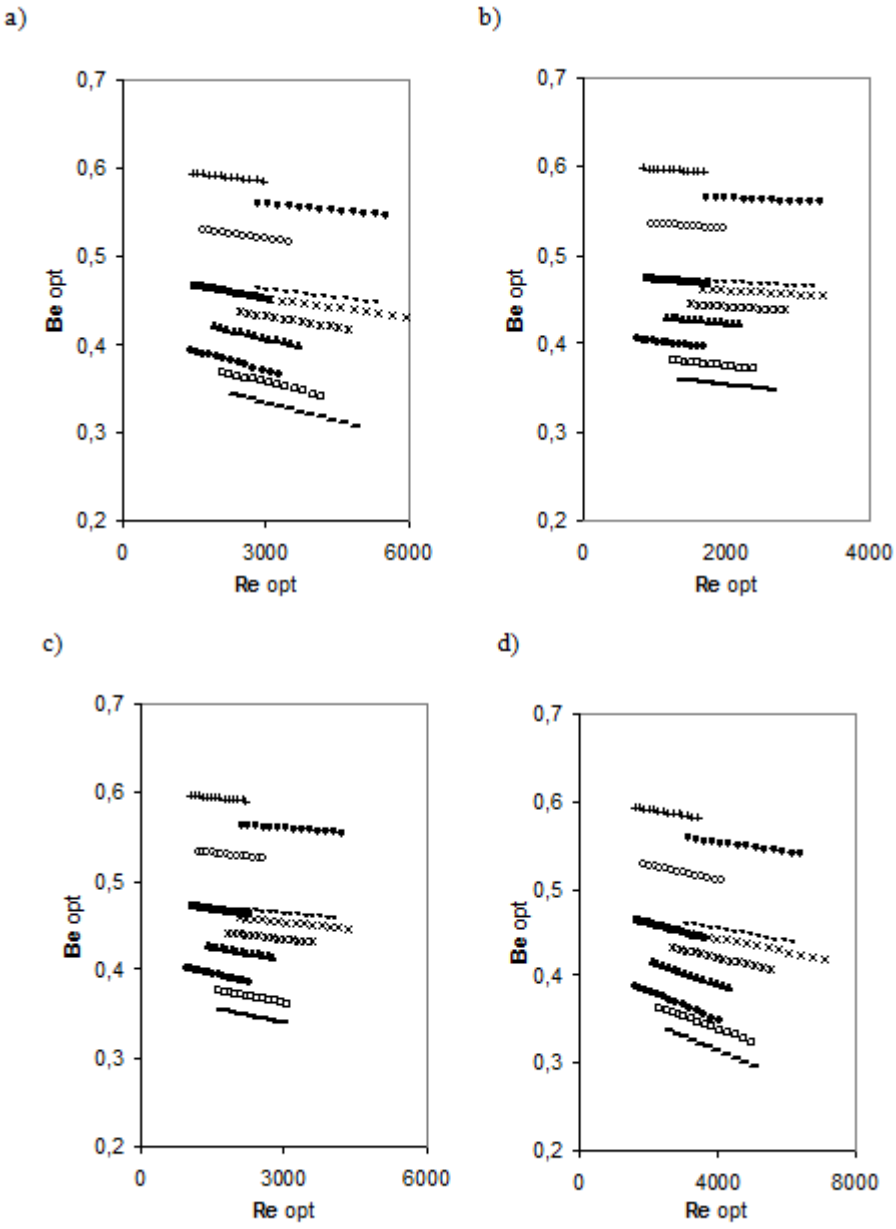

Fig. 3.2. Dependence of optimal Bejan number (Be_{opt}) on the Reynolds number through the eleven carriers under conditions of variable pressure at outlet air. The carrier description are presented in table 1.1 and in fig. 2.1. The carrier description are presented in table 1.1 and in fig. 2.1. The process parameters are given by legend of fig. 2.1., however inlet air temperature was changed successively for: a)335K, b)355K; or tube wall temperature was changed successively for: c) 358K, d)378K.

and simultaneously, the optimal Re_{opt} values grow. The maximal Be_{opt} values were obtained for carriers no. 7 and 6. The curves 1 and 11 intersect each other. In that case, at the lower pressure the carrier no. 1 show higher value of Be_{opt} , however at the elevated pressure such relation becomes inverted.

Calculations were made for the values of Be_{opt} and Re_{opt} under the process parameter condition from table 3.1. These calculation results are presented in figs. 3.1 – 3.2. It can be seen with these figures that an increase of the

bed length results in low increase of Be_{opt} values , and, simultaneously, in considerable reduction of Re_{opt} values. The same influence on the Be_{opt} and Re_{opt} values exerts raising of the inlet air temperature.

Calculations for the values of Be_{opt} and Re_{opt} were performed as well, in dependence with the process parameters collected in table 3.2. As a result, a large, over 600 points data-base have obtained. This data-base was made to develop the above-type relationships of the process parameters area.

4. Correlations between optimal Reynolds number, optimal Bejan number, dimensionless term Nu/S'''_{max} and the process parameters

Calculated values of the Be_{opt} and Re_{opt} numbers were correlated with the process parameter data.

Thus, the following correlation (4.1) was obtained for Be_{opt} values under the process parameter conditions given bellow (4.2).

$$Be_{opt} = \alpha_o (L/L_o)^{\alpha} (P/P_o)^{\beta} (T_{in}/T_{in,o})^{\gamma} (T_w/T_{w,o})^{\delta} \tag{4.1}$$

Where: L_o =0.6m, P_o= 1, $T_{in,o}$=315K and $T_{w,o}$=398K. (4.2)

Also, an analogous correlation was obtained for Re_{opt} values under the above process parameter conditions

$$Re_{opt} = a_o (L/L_o)^{a} (P/P_o)^{b} (T_{in}/T_{in,o})^{c} (T_w/T_{w,o})^{d} \tag{4.3}$$

Completing, a correlation for dimensionless term Nu/S'''_{max} was determined

$$Nu/S'''_{max} = A_o (L/L_o)^{A} (P/P_o)^{B} (T_{in}/T_{in,o})^{C} (T_w/T_{w,o})^{D} \tag{4.4}$$

Values of the constants α, β, γ and δ for in the correlation (4.1) for Be_{opt} established within the 11 carriers are given in table 4.1. Next, values of the constants a_0 ,a, b, c, d, and A_0, A, B, C, D in correlation (4.3) for Re_{opt} , and in correlation (4.4) for Nu/S'''_{max} , respectively, were established within the eleven carriers, as well. They are in tables 4.2 and 4.3, respectively.

Table 4.1. Power expressions in correlation (4.1) for values of Be_{opt}

Carrier No.	α_o	α	β	γ	δ
1	0.437568	0.532193	-0.0529768	0.500663	-0.476078
2	0.44429	0.0277283	-0.0425642	0.551077	-0.533413
3	0.384614	0.0603975	-0.0776422	0.971181	-0.851426
4	0.418423	0.0774294	-0.0587184	0.755395	-0.72651
5	0.541106	0.0579063	-0.0537808	0.175237	-0.0537808
6	0.438945	0.0139406	-0.109057	0.88597	-0.909555
7	0.58252	0.0362071	-0.218929	0.228085	-0.0417397
8	0.43894	0.0816419	-0.758619	0.756101	-0.114959
9	0.257854	0.200309	-0.0984238	2.91137	-2.86227
10	0.514701	0.0277283	-0.0425642	0.551077	-0.533413
11	0.31953	0.106886	-0.0897739	1.4843	-1.44029

Table 4.2. Power expressions in correlation (4.3) for values of $Re_{opt.}$

Carrier No.	a_o	a	b	c	d
1	3477	-1.59976	1.79368	-9.87882	8.99826
2	3111	-1.28573	1.25999	-6.36484	5.58938
3	3803	-1.0589	1.53376	-5.52242	5.14623
4	6094	-1.27582	1.33073	-7.96435	7.57024
5	4828	-1.16274	1.0123	-7.28815	6.70694
6	5530	-1.12408	1.24843	-6.67886	6.00101
7	2921	-1.28573	1.25999	-6.36484	5.58938
8	5333	-1.05068	1.01034	-6.92323	5.53958
9	5712	-1.32264	1.39457	-9.98819	9.58934
10	3459	-1.31094	1.39934	-7.36328	6.60939
11	4449	-1.04698	1.10355	-7.58772	6.88118

Table 4.3. Power expressions in correlation (4.4) for values of Nu/S'''_{max}

Carrier No.	A_o	A	B	C	D
1	2810	-0.261439	1.1788	4.14587	-4.73544
2	3873	-0.088147	1.03641	4.98838	-5.52493
3	3119	-0.192022	1.11181	4.44735	-5.02697
4	4519	-0.14649	1.05346	4.84905	-5.40638
5	4567	-0.171579	1.12402	4.51627	-5.04767
6	4958	-0.023788	0.872838	6.11595	-6.52278
7	5763	-0.152356	0.812436	6.44268	-6.80224
8	5300	-0.12881	1.06235	4.90868	-5.41313
9	3319	-0.355441	1.26304	3.40441	-4.03865
10	4210	-0.004813	0.92879	5.73568	-6.17305
11	3752	-0.29429	1.23287	3.92483	-4.52355

Evaluation of the Re_{opt} value from correlation (4.3) was compared with an additional calculation from the exact values of the process parameters that are given in tables 3.1 – 3.2. Fig. 4.1 shows this comparison results as the parity relation. This can be seen in fig. 4.1, that the parity is satisfactory. Moreover, evaluations of Be_{opt} and Nu/S'''_{max} values from correlations (4.1) and (4.4), respectively, were compared with their calculations from exact values of the process parameters given in tables 3.1 – 3.2. Also the correlations 4.1 and 4.4 accurately describe the values of Be_{opt} and Nu/S'''_{max}.

5. Final conclusions

Along with the variable controlled previously , knowledge of the optimal Bejan number values was indicated to be necessary for determination of optimal work conditions of the catalyst carriers and other structured fillings within the above mentioned process area. The optimal Bejan number values for which ratio of Nusselt number values to the

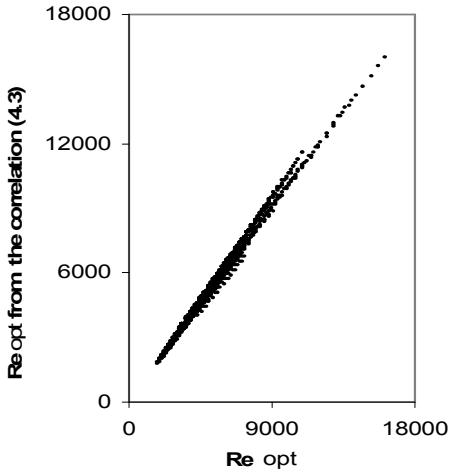

Fig. 4.1. Parity plot comparing Re_{opt} values with the prediction of correlation (4.3).

dimensionless entropy generation rate reached its maximal value were introduced in this work. Relevant calculations were performed within the eleven selected catalyst carriers while the bed length, the outlet air pressure, the inlet air and the tube wall temperatures were changed successively.

In all, a set of 481 values of the optimal Bejan number Be_{opt} were determined for each case of the eleven catalyst carriers. These determination results are plotted in figs. 2.2b – 3.2. The carriers can be settled according to the growing values of Bejan number. In these figures, Be_{opt} values change in a range from 0.2 to 0.6. The highest Be_{opt} values were determined for carriers no. 7 and no. 6, while the lowest ones for carriers no. 9 and no. 11.

With increase of the dimensionless outlet air pressure, the optimal Bejan number decrease while the optimal Reynolds number increase. For the low-value Be_{opt} carriers, a considerable increase of both these numbers was observed while increase the bed length, the inlet air temperature or the tube wall temperature. In a turn, in a case of high-value Be_{opt} carriers these numbers increase slightly. As can be seen in fig. 2.2b, the curves for carrier 1 and carrier 2 intersect each other. For lower pressure values, carrier no. 11 has lower Be_{opt} values, however, for higher pressure values this dependence changes. Therefore, optimal work conditions for the catalyst carriers can depend on the process parameter values.

The correlations of the optimal Bejan number values were determined for the eleven catalyst carriers in dependence on the four essential parameters of the process. These correlations are given in table 4.1.

Next, in tables 4.1 and 4.3 correlations with optimal Reynolds number values and the maximal Nu/S'''_{max} ratio values are listed, respectively. Deviation of the Re_{opt} number values calculated with the correlation 4.3 from the analogous values calculated with the exact process parameter data are presented in fig. 4.1. This figure shows that these calculation results are in good agreement with one another. Therefore, on the basis of these correlations characterized in tables 4.1 – 4.3, determination of the optimal work conditions for the catalyst carriers and similar structured fillings can be performed quickly and simply, and this approach can be generalized for relevant engineering designs.

6. Nomenclature

a	specific surface, m^2/m^3
Be	Bejan number
c_p	specific heat, J/(kg·K)
D	tube diameter, m

F Fanning friction factor
G mass velocity, kg/m^{2}s
j Colburn factor
L tube length, m
$\dot{m}$ mass flow rate, kg/s
Nu Nusselt number
Re Reynolds number
Nu/ $\dot{S}$ ''' proportion of Nusselt numer to dimensionless entropy generation rate
Nu/S''' $_{max}$ maximum of Nu/ $\dot{S}$ ''' value
P=p/p_o (p_o=101.325 kPa) dimensionless pressure
p pressure, Pa
q heat flux, W
Re=GD/η Reynolds number
Re_{opt} Reynolds number for Nu/S''' $_{max}$
$\dot{S}$ entropy generation rate, W/K
$\dot{S}$ '''= $\dot{S}$ /($\dot{m}$ c_p) dimensionless entropy generation rate
St Stanton number
T_{in} inlet air temperature, K
T_m gas mean temperature, K
T_w tube wall temperature, K
ε porosity
η viscosity, Pa.s
ρ gas density, kg/m^3

References

1. *Structured Catalysts and Reactors*, eds. Cybulski A., Moulijn J. A., Taylor&Francis, Boca Raton 2006
2. Kolodziej A., Krajewski W., Dubis A., *Cat. Today,* 69(1-4), 2001, 115-120
3. Chrząszcz J., Krajewski W., Kołodziej A., Dubis A, *Inż. Chem. Proc*., 22, 2001, 337-342
4. Krajewski W., Matysik S., Najzarek Z., Dubis A., *Arch. Ochr. Środ.*, 25, 1999, 55-59
5. Shuja S. Z., Zubair S. M., Khan M. S., *Heat and Mass Transfer*, 34, 1999, 357-364
6. Shah R.K., Seculic D.P, *Fundamentals of Heat Exchangers Design*, Wiley, New Jersey 2003